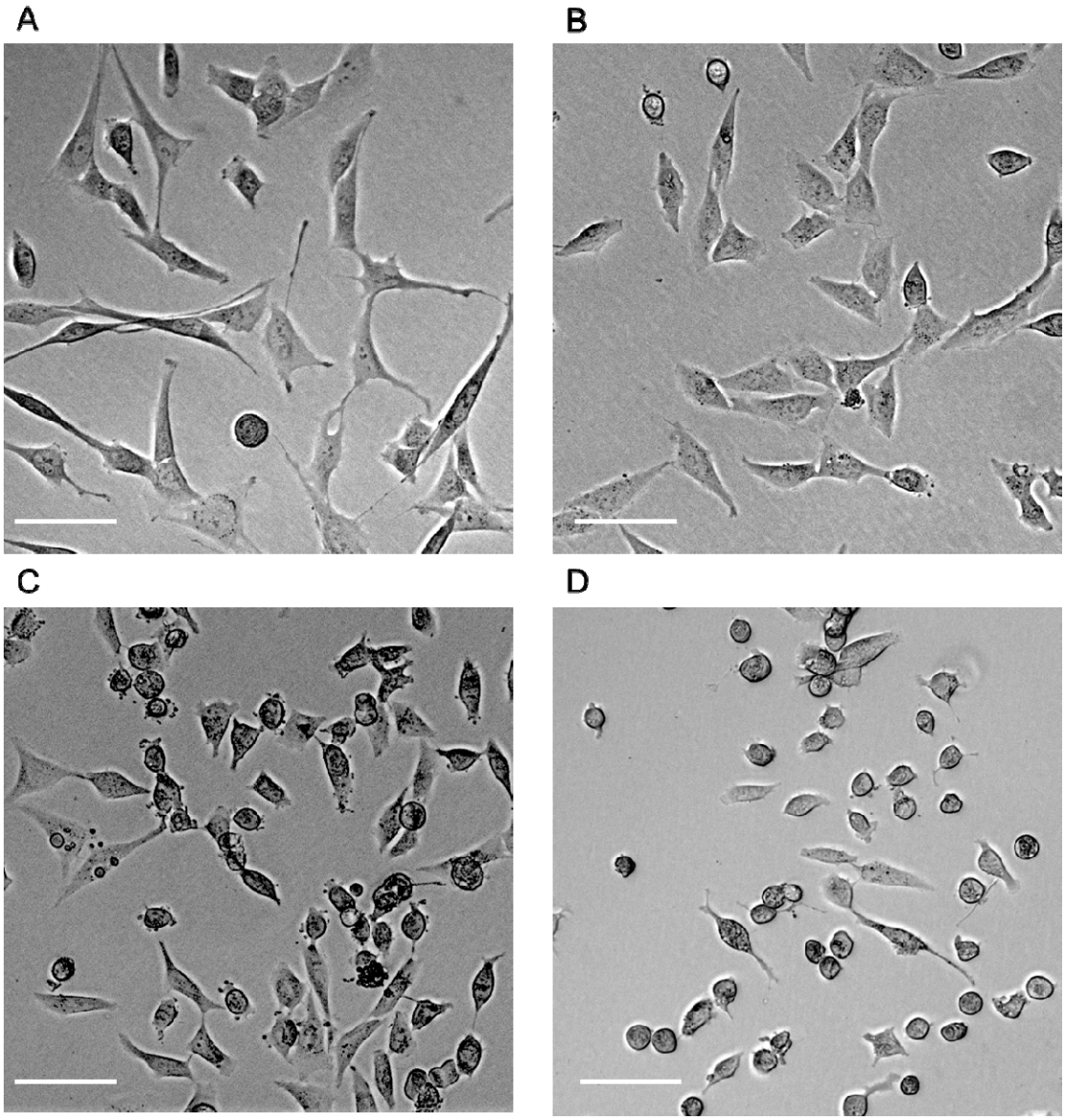

Figure S1: Cell morphology after exposure to nanoparticles. Cells were treated with 50 μg ml^{-1} NH_2-PS NPs in cDMEM for 0 h (A, untreated control), 6 h (B), 8 h (C) and 24 h (D). Phase contrast images were taken using a Zeiss Axiovert inverted microscope in order to monitor changes in cell morphology, which could indicate cell damage. After 6 and 8h exposure, clear changes in cell phenotype could be observed in some of the cells, as a sign of cell death, while other cells were similar to untreated cells. As discussed in the Manuscript, these images suggest heterogeneity in the response to NH_2-PS NPs for individual cells within the same population. Scale bar: 100 μm.

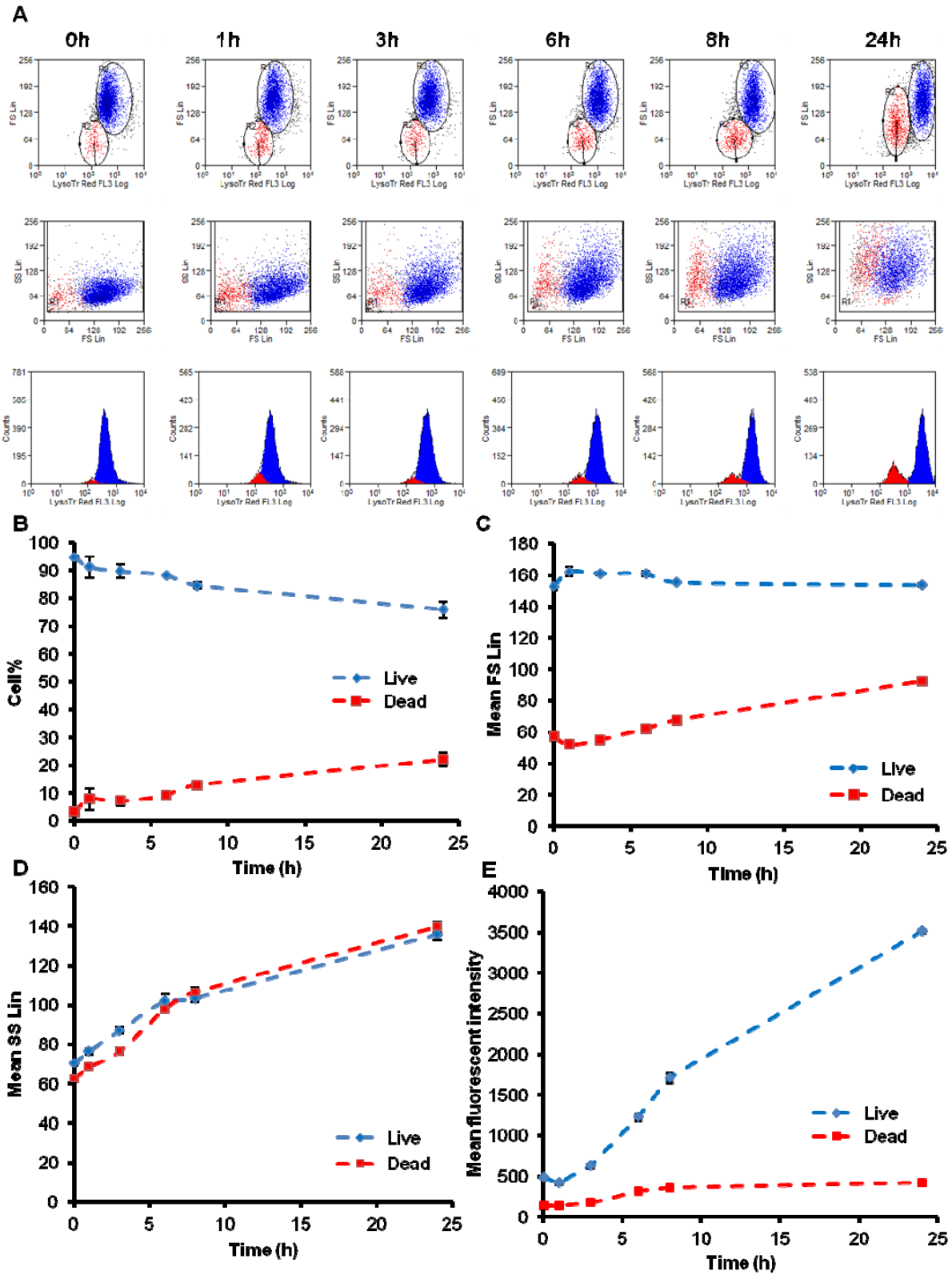

Figure S2: Lysosomal staining by flow cytometry with LysoTracker Red. Cells were treated with 50 μg ml^{-1} NH_2-PS NPs for indicated times (0h untreated, 1h, 3h, 6h, 8h and 24h) and stained with 50 nM LysoTracker Red as described in the Experimental section. **A.** Distributions of LysoTracker Red staining. Top panel: forward scatter (FS Lin) *versus* LysoTracker Red fluorescence intensity. The dot plots show two distinguished populations -

one with higher LysoTracker Red intensity and higher FS Lin (gate R3, blue), and one with lower LysoTracker Red intensity and lower FS Lin (gate R2, red). The same gates and colour codes were applied to the dot plots of side scatter (SS Lin) *versus* forward scatter (FS Lin) (middle panel) and the distributions of LysoTracker Red fluorescence intensity (bottom panel). This analysis suggests that the blue population contains cells with lysosomes stained by LysoTracker Red and regular cell size, while the red population contains cells with loss of lysosomal staining or in late stage of cell death. At later exposure times (6h, 8h and 24h) an increase in LysoTracker Red intensity was observed, together with an increase of SS Lin (cell granularity) which indicates increased volume of acidic compartments and of the degree of vacuolization. **B.** Percentage of cells in the two subpopulations (blue and red, as defined in panel A) as a function of time, showing increasing percentage of cells with loss of lysosomal staining (red). **C-E.** Mean forward scatter (FS, C), side scatter (SS, D) and LysoTracker Red intensity (E) as a function of time for the cells in the two sub-populations (blue and red, as defined in panel A). The FS data (C) shows that dead cells (red) have lower FS compared to the main cell population (blue). The SS data (D) shows increase of SS after treatment with NPs, which suggests an elevated degree of vacuolization in the cells in response to the NPs. The results for LysoTracker Red (E) confirms increase of staining in the main cell population (blue) which indicates increasing volume of acidic compartments, while at later exposure time an increased number of cells with low staining is observed (red). Error bars are the standard deviation among 3 replicates. Panel A is reproduced from ref. 9 (Wang *et al. Nanomedicine NBM*, 2013).

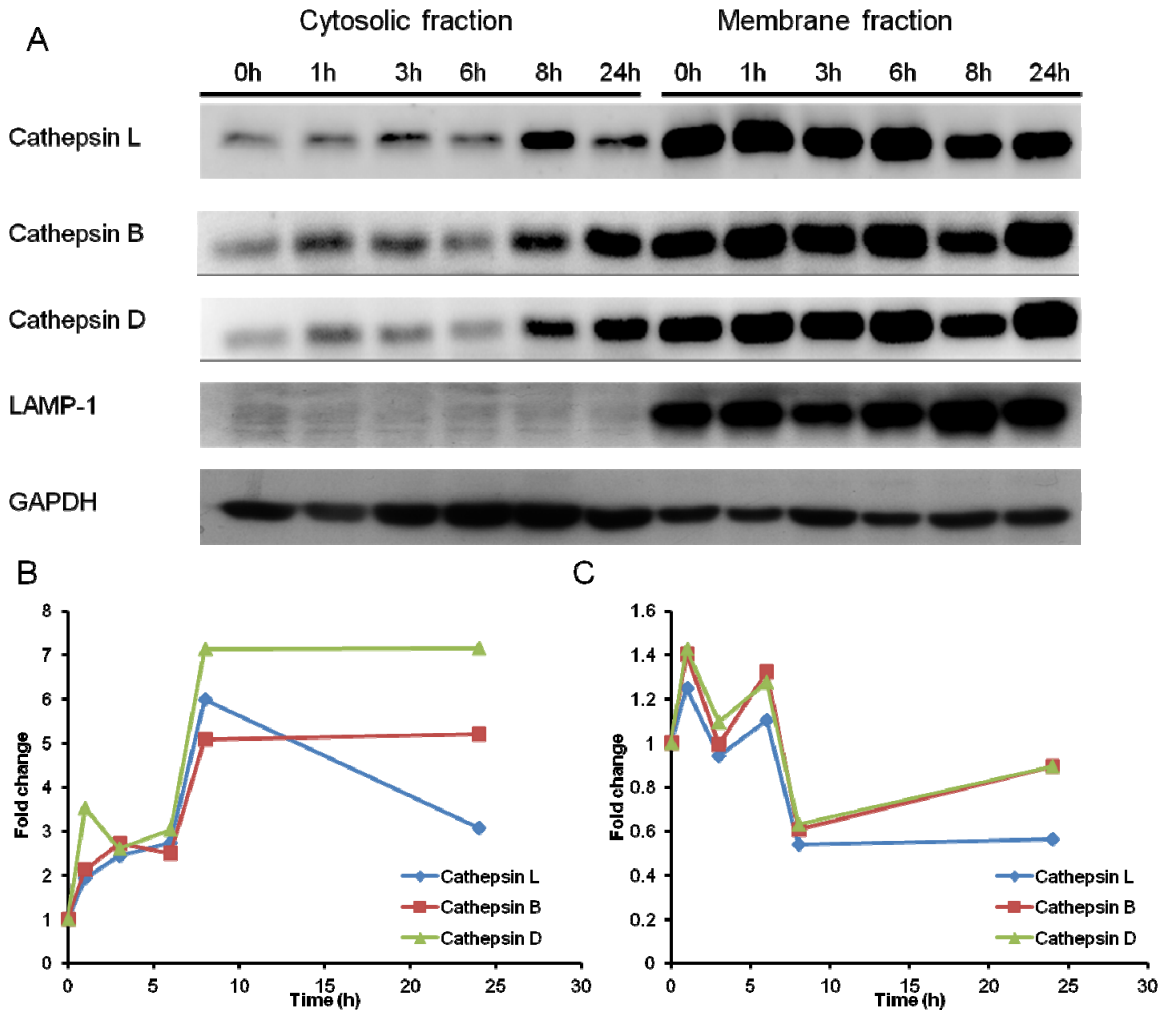

Figure S3: Western blot of cathepsins release from lysosomes to cytosol. Cells were treated with 50 μg ml^{-1} NH_2-PS NPs for indicated times (0h untreated, 1h, 3h, 6h, 8h and 24h). Cytosolic and membrane (organellar) fractions of the cells were separated as described by Oberle *et al* (*Cell Death Differ* 2010;**17**:1167-1178). **A.** Western blot of the cytosolic and membrane fractions for cathepsins L (Cat L, 25kDa), B (Cat B, 30kDa), and D (Cat D, 28kDa) showing the release of these three cathepsins from lysosomes to cytosol after 8h exposure to nanoparticles. LAMP1 staining confirms that no lysosomes were present in the isolated cytosolic fractions. GAPDH was used as a loading control. **B and C.** Densitometry analysis of the cytosolic (B) and membrane (C) amounts of Cat B, D and L. The intensity of each band was first normalized by the intensity of the GAPDH band in the same sample (loading control). Then the results were normalized by the value obtained for untreated control cells in order to determine the difference in protein levels in respect to untreated cells (Fold change).

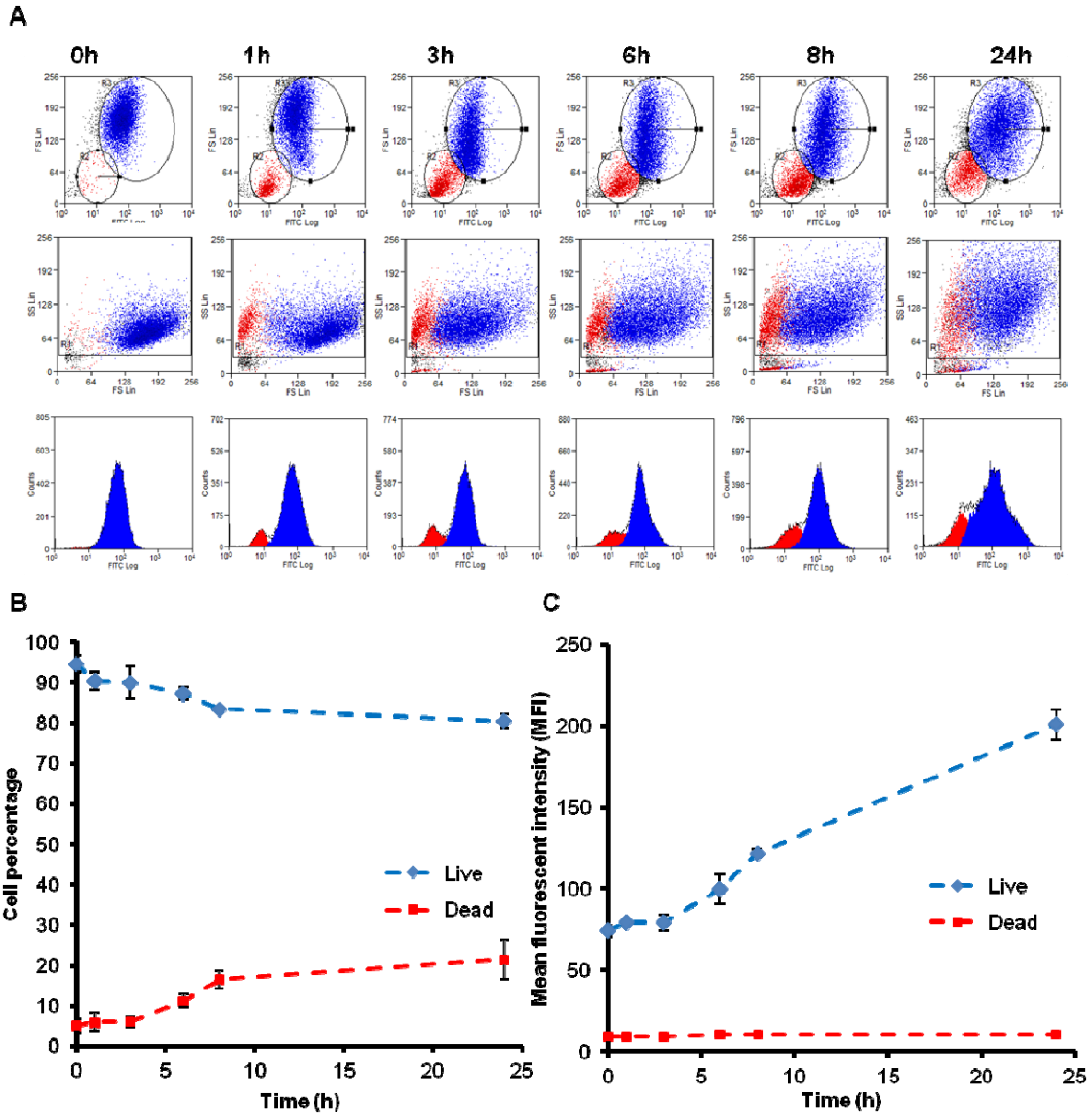

Figure S4: Flow cytometric analysis of ROS generation by CM-H_2DCFDA staining. Cells were treated with 50 µg ml^{-1} NH_2-PS NPs for indicated times (0h untreated, 1h, 3h, 6h, 8h and 24h), and stained with 2.5 µM CM-H_2DCFDA as described in the Experimental section. **A.** Flow cytometric distributions of CM-H_2DCFDA staining. Top panel: FS Lin *versus* CM-H_2DCFDA fluorescence intensity. The dot plots show two distinguished populations - one with higher CM-H_2DCFDA fluorescence intensity and higher FS Lin (gate R3, blue), and one with lower CM-H_2DCFDA fluorescence intensity and lower FS Lin (gate R2, red). The same gates and colour codes were applied to the dot plots of SS Lin *versus* FS Lin (middle panel) and the distributions of CM-H_2DCFDA fluorescence intensity (bottom panel). This analysis shows an increasing generation of ROS in the main cell population (blue) at increasing exposure time, while cells in late stage of cell death are not stained by the dye (red). **B.** Percentage of cells in the two subpopulations (blue and red, as defined in panel A) as a function of time. **C.** Mean fluorescence intensity (MFI) of CM-H_2DCFDA as a function of time, for cells in the two subpopulations (blue and red, as defined in panel A). The plot shows increase of CM-H_2DCFDA intensity in the main cell population (blue), which indicates increasing amount of ROS is generated at increasing exposure time. Error bars are the standard deviation among 3 replicates.

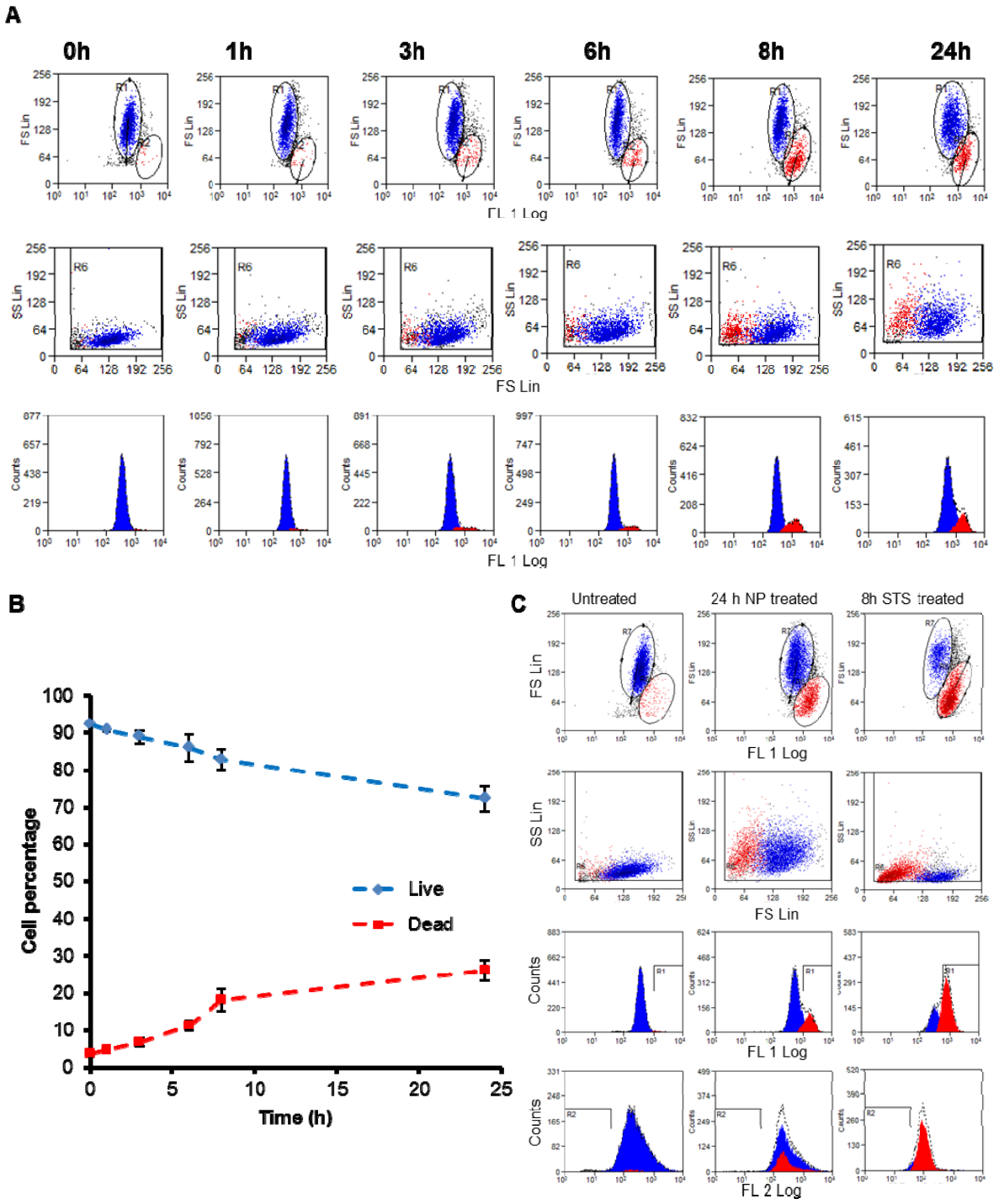

Figure S5: Flow cytometric analysis of mitochondrial membrane potential by JC-1 staining. Cells were treated with 50 µg ml^{-1} NH_2-PS NPs for indicated times (0h untreated, 1h, 3h, 6h, 8h and 24h) and stained with 1 µg/ml JC-1 as described in the Experimental section. **A.** Flow cytometric distributions of JC-1 staining in FL1 (530/40 nm) channel. Top panel: FS Lin *versus* JC-1 FL1 fluorescence intensity. The dot plots show two distinguished populations - one with lower fluorescence intensity and higher FS Lin (gate R3, blue), and one with higher JC-1 FL1 fluorescence intensity and lower FS Lin (gate R2, red). The same gates and colour codes were applied to the dot plots of SS Lin *versus* FS Lin (middle panel) and the distributions of JC-1 FL1 fluorescence intensity (bottom panel). This analysis

suggests that the blue population is constituted by cells that maintain mitochondrial membrane potential and regular cell size, while the red population represents cells that have lost their mitochondrial membrane potential. **B.** Percentage of cells in the two sub-populations (blue and red, as defined in panel A) as a function of time. This plot shows increasing percentage of cells with loss of mitochondrial potential at increasing exposure time. Error bars are the standard deviation among 3 replicates. **C.** Analysis of JC-1 red and green fluorescence (as recorded in FL1 and FL 2 channels, respectively) for untreated control cells, 24h NP treated cells and cells treated with 1 μM staurosporine (STS) for 8h. STS is a common positive control known to induce loss of mitochondrial membrane potential. This causes a decrease in red fluorescence signal of JC-1 and an increase in its green fluorescence. The results obtained with this system in the two channels were compared in order to define best ways to analyse data. In this case we observed that the increase of FL1 green fluorescence allowed a better separation of subpopulation of cells with loss of mitochondrial potential. For this reasons results were analysed in the green fluorescence channel.

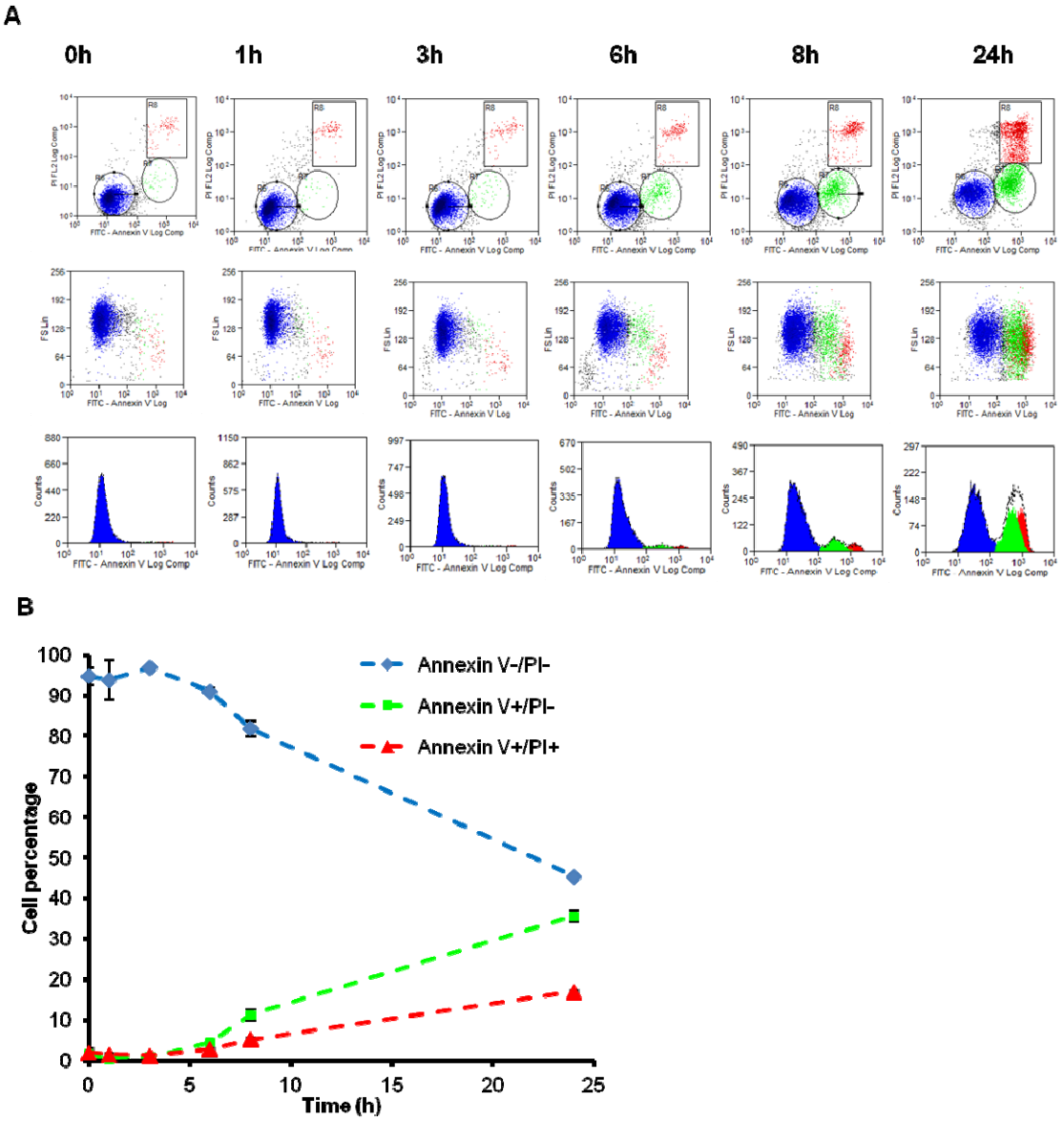

Figure S6: Flow cytometric analysis of plasma membrane integrity and cell death by annexin V and propidium iodide (PI) double staining. Cells were treated with 50 μg ml^{-1} NH_2-PS NPs for indicated times (0h untreated, 1h, 3h, 6h, 8h and 24h), and stained with annexin V- FITC and PI as described in the Experimental section. **A.** Flow cytometric distributions of annexin V- FITC and PI double staining. Top panel: PI fluorescence intensity versus annexin V- FITC fluorescence intensity. The dot plots show three distinguished populations - double negative (gate R6, blue, healthy cells), annexin V positive and PI negative (gate R7, green, early apoptotic cells) and double positive (gate R8, red, late apoptotic and necrotic cells). The same gates and colour codes were applied to the dot plots of forward scatter (FS Lin) *versus* annexin V- FITC fluorescence intensity (middle panel) and distributions of annexin V- FITC fluorescence intensity (bottom panel). **B.** Percentage of cells in the three cell sub-populations (blue, green and red, as defined in panel A) as a function of time. Annexin V/PI staining shows a steady increase in the percentage of early apoptotic cells (green) and cells in late stage of cell death (red, late apoptotic/necrotic cells) at increasing

exposure times, which is mirrored by a steady decrease in the fraction of healthy cells (blue, double negative stained cells). Error bars are the standard deviation among 3 replicates.

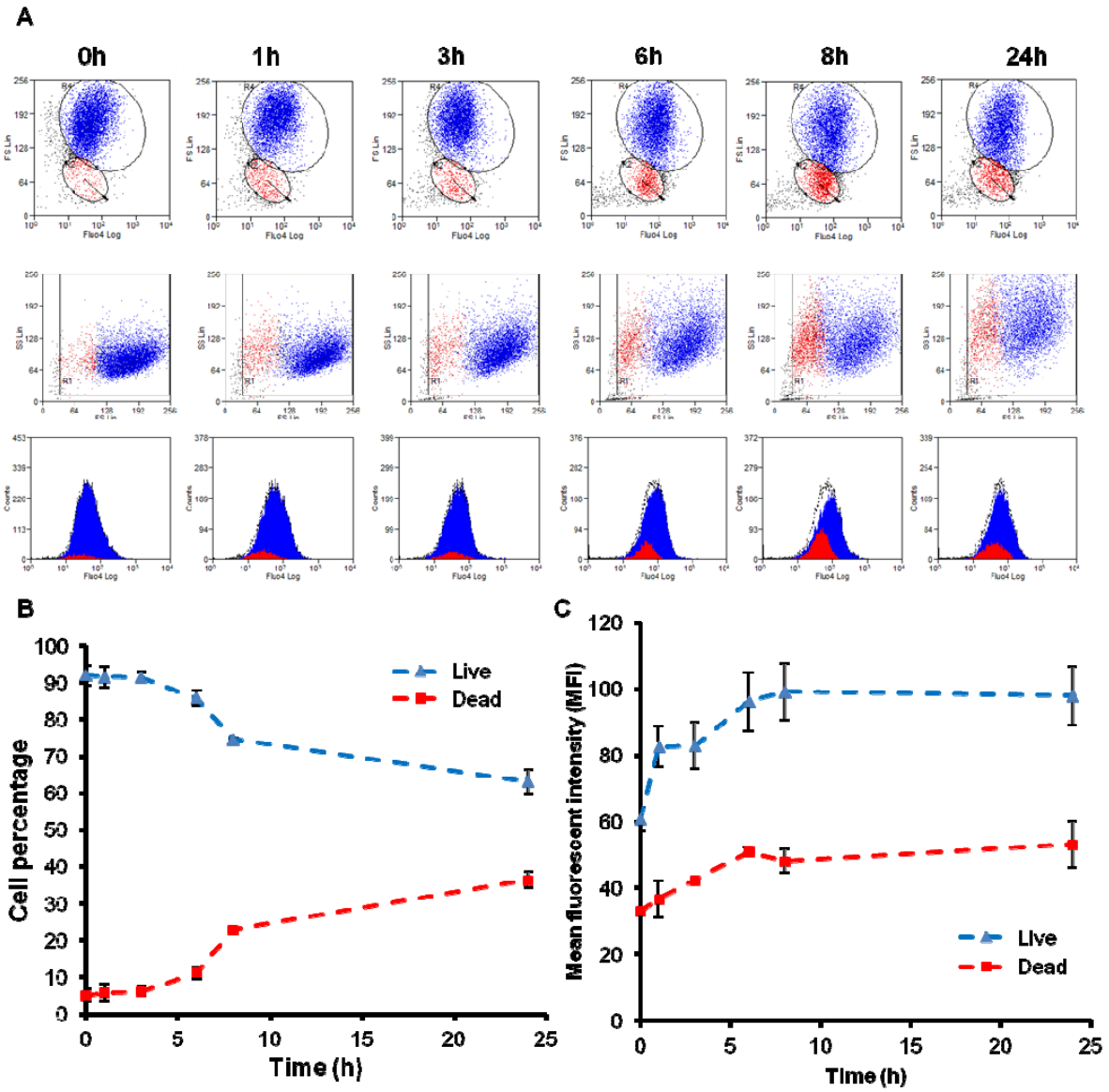

Figure S7: Flow cytometric analysis of intracellular calcium by Fluo 4 staining. Cells were treated with 50 µg ml^{-1} NH_2-PS NPs for indicated times (0h untreated, 1h, 3h, 6h, 8h and 24h), and stained with 3 µM Fluo 4 at 37˚C for 20 min in dark and measured immediately by flow cytometry (excitation: 488 nm laser; emission filter: FL 1 530/40 nm channel). **A.** Distributions of Fluo 4 staining. Top panel: FS Lin *versus* Fluo 4 fluorescence intensity. The dot plots show two distinguished populations - one with higher Fluo 4 fluorescence intensity and higher FS Lin (gate R4, blue), and one with lower Fluo 4 intensity and lower FS Lin (gate R2, red). The same gates and colour codes were applied to the dot plots of SS Lin *versus* FS Lin (middle panel) and the distributions of Fluo 4 fluorescence intensity (bottom panel). **B.** Percentage of cells in the two sub-populations (blue and red, as defined in panel A) as a function of time. **C.** Fluo 4 mean fluorescence intensity (MFI) of the two cell sub-populations (blue and red, as defined in panel A) as a function of time. The plot shows increasing amount of intracellular calcium in the main cell population (blue) after exposure to NPs. Error bars are the standard deviation among 3 replicates.

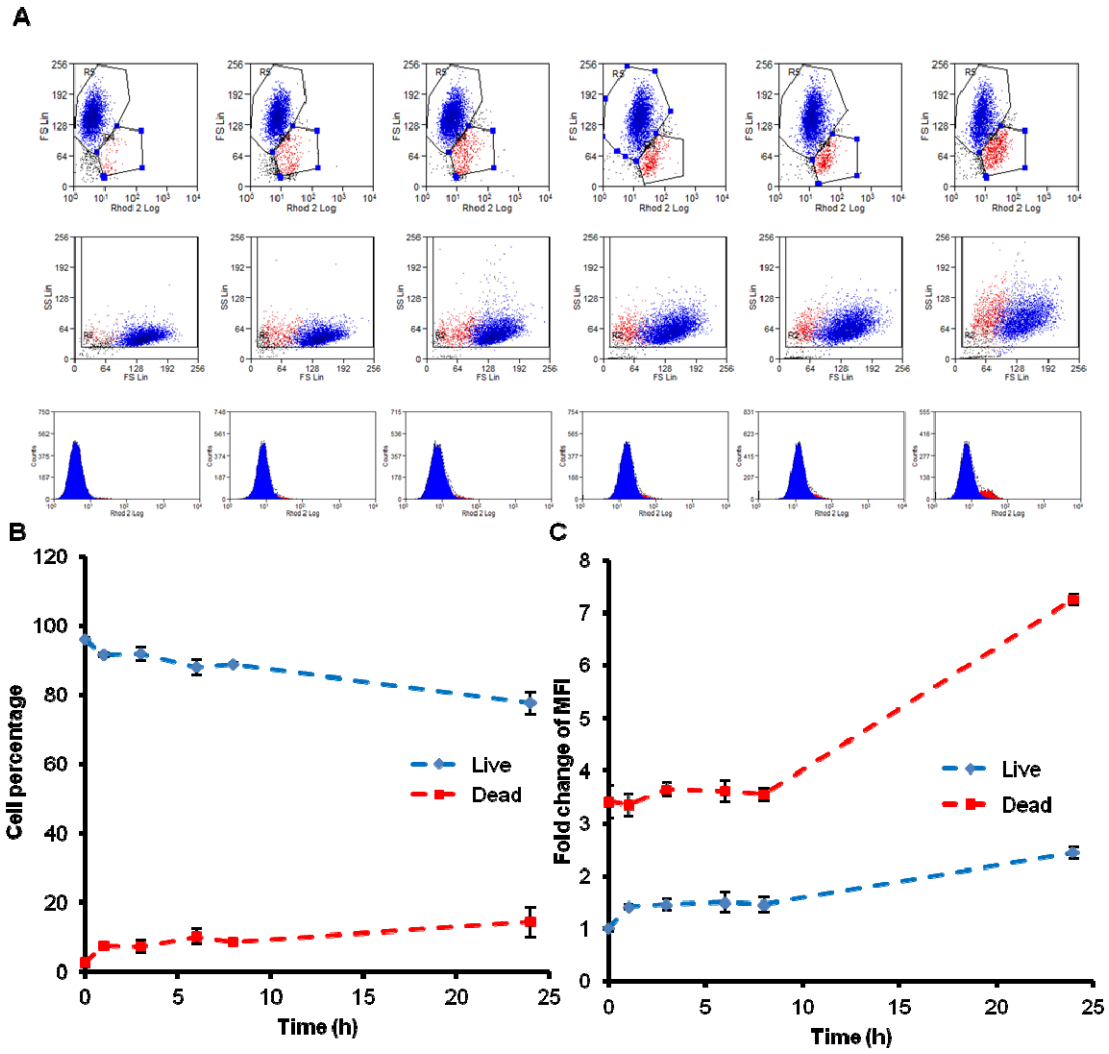

Figure S8: Flow cytometric analysis of mitochondrial calcium by Rhod 2 staining. Cells were treated with 50 μg ml^{-1} NH_2-PS NPs for indicated times (0h untreated, 1h, 3h, 6h, 8h and 24h), and stained with 3 μM Rhod 2 at 37˚C for 20min in darkness and measured immediately by flow cytometry (excitation: 488 nm laser; emission filter: FL 1 530/40 nm channel). **A.** Distributions of Rhod 2 staining. Top panel: FS Lin *versus* Rhod 2 fluorescence intensity. The dot plots show two distinguished populations - one with lower Rhod 2 intensity and higher FS Lin (gate R5, blue), and one with higher Rhod 2 intensity and lower FS Lin (gate R4, red). The same gates and colour codes were applied to the dot plots of SS Lin *versus* FS Lin (middle panel) and the distributions of Rhod 2 fluorescence intensity (bottom panel). **B.** Percentage of cells in the two sub-populations (blue and red, as defined in panel A) as a function of time. **C.** Rhod 2 mean fluorescence intensity (MFI) for cells in the two sub-populations (red and blue, as defined in panel A) as a function of time. The values were normalized by the MFI of untreated control cells at each time. The main cell population (blue) shows slight increase of mitochondrial calcium levels, with around 2 fold increase at 24h. Cells in the red sub-population show higher mitochondrial calcium level than blue cells, as those cells were at late stage of cell death. Error bars are the standard deviation among 3 replicates.

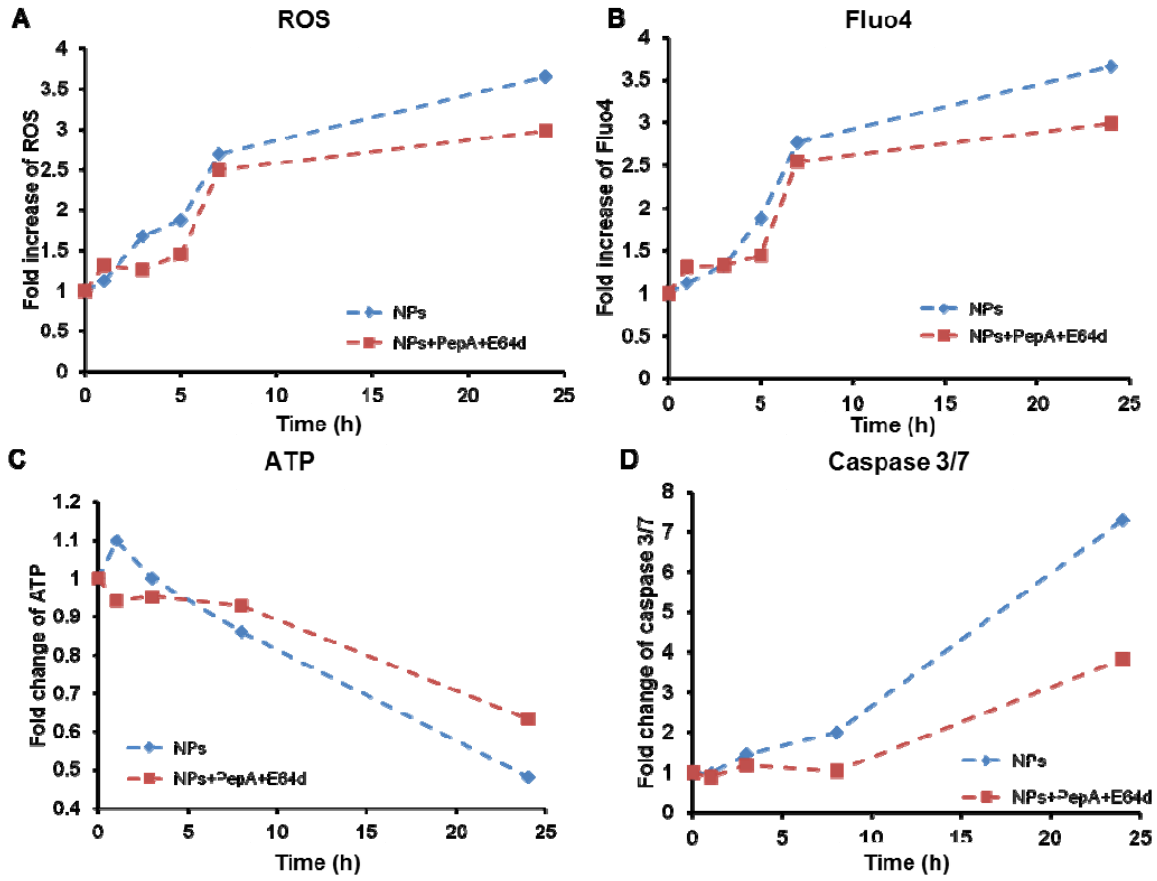

Figure S9: Role of cathepsins in the observed cell death. Cells were treated with 50 µg ml^{-1} NH_2-PS NPs for indicated times with or without pre-incubation with cathepsin inhibitors (50 µM PepA and 30 µM E64d), followed by measurement of ROS levels by CM-H_2DCFDA (A), intracellular calcium levels by Fluo 4 (B), ATP (C) and Caspase 3/7 activation (D) as previously described. The blue lines show the results for cells treated with NPs only; the red lines show the results for cells treated with the NPs in the presence of the two different inhibitors (Pep A and E64d). All plots have been normalised by the mean fluorescence intensity of control cells not exposed to the NPs, but treated in the same way (without and with inhibitors, respectively, for the blue and red lines). The inhibition of cathepsins can slightly decrease the level of ROS and intracellular calcium. At the same time, the inhibition of cathepsins reduces slightly cell death and decreases caspase 3/7 activation. These results overall suggest that the release of cathepsins is an important step in the mechanism of cell death induced by these NPs.